Developmental and Comparative Immunology 33 (2009) 709–717

Contents lists available at ScienceDirect

Developmental and Comparative Immunology

journal homepage: www.elsevier.com/locate/dci

Identification and functional characterization of a novel cytidine deaminase in a gastropod abalone, *Haliotis diversicolor supertexta*

Liuji Wu, Xinzhong Wu *, Baojian Zhu, Xiaohua Cao

Laboratory of Marine Life Science and Technology, College of Animal Sciences, Zhejiang University, 268 Kaixuan Road, Hangzhou 310029, PR China

ARTICLE INFO

Article history:
Received 22 October 2008
Received in revised form 18 December 2008
Accepted 18 December 2008
Available online 16 January 2009

Keywords:
Abalone *Haliotis diversicolor supertexta*
Cytidine deaminase
Biological activity
Intracellular localization
Immune response

ABSTRACT

Cytidine deaminase (CDA, also designated CDD) is a zinc-dependent enzyme involved in the pyrimidine salvage pathways and becoming very important in anticancer and antiviral therapy. Here we report the identification and characterization of a CDA homologue in abalone, which we named ab-CDA. The analysis of the amino acids sequence revealed that the ab-CDA shares conserved signature motifs and belongs to homotetrameric class of CDA family. Real-time PCR analysis indicated that the ab-CDA was ubiquitously expressed in various tissues of abalone and relatively higher expressed in hemocyte. Significant up-regulation of ab-CDA was also observed after LPS or Poly I: C challenge. The biological activity of ab-CDA was identified by spectrophotometry analysis and the intracellular localization displayed that ab-CDA was largely concentrated in the cytoplasm and partially in the nuclei. These results strongly suggest that ab-CDA is a CDA homologue and it is involved in the immune response of gastropod abalone.

© 2009 Elsevier Ltd. All rights reserved.

1. Introduction

Cytidine deaminase (CDA) is a salvage pathway enzyme catalyzing the hydrolytic deamination of cytidine (CR) and deoxycytidine (CdR) to the corresponding uracil nucleosides [1–4]. CDA also plays an important role in the metabolism of a number of antitumoral and antiviral cytosine nucleoside analogs, causing their pharmacological inactivation [5,6].

Based on crystal structures and deduced amino acid sequences of CDAs from different species, CDAs have been organized into two classes. One is the homodimeric class, such as *Escherichia coli* CDA [7], *Arabidopsis thaliana* CDA [8] and *Haemophilus influenzae* CDA [9]. Homodimeric CDA consists of two symmetrical (2×31.5 kDa) monomers, each monomer has a molecular weight of about 31 kDa and contains three domains: a small N-terminal domain, a catalytic domain equipped with a zinc atom and a C-terminal domain. The other is the homotetrameric class, such as *Bacillus subtilis* CDA [10], human CDA [11,12] and chicken CDA [13]. A high level of structural conservation is observed between the homotetrameric members, although they do not have high identity at the amino acid level [11]. The homotetramer is known biochemically to be the functional unit of human CDA which has 2-fold symmetry [1]. The homotetrameric CDA monomer has a molecular weight of approximately 15 kDa which is structurally similar to the catalytic domain of the *E. coli* CDA. Each of the four subunits links an essential zinc atom coordinated with three negatively charged cysteine residues: C65, C99 and C102 [10,11]. The zinc is essential for the enzymatic activity and the active site of one monomer is formed by the contribution of residues coming from the other three monomers [14]. In addition, there is a special family of CDA called mammalian APOBEC3 (Apolipoprotein B Mrna-Editing enzyme catalytic polypeptide-like editing complex 3). Mammalian APOBEC3 includes several members that possess potent antiretroviral activity [15,16] by acting through CDA enzymatic activity and though less-well-understood nonenzymatic nechanisms [17].

Abalone is an important mollusc species for commercial production in the world including Australia, China, Japan, Korea, Mexico, South Africa, and the United States [18]. Since the late 1990s, the global industry of abalone has been gradually decreased due to diseases and environmental pollution [19,20]. Therefore, more investigation is required to aid in understanding the innate immune system of abalone for aquaculture development.

CDA-related genes have been reported in several mollusc species. For example, Bouchut et al. [21] showed that *biomphalaria glabrata* CDA (DQ117977) is differentially represented in hemocytes between susceptible and resistant strains to the parasite, *Echinostoma caproni* at the protein level. Boutet et al. [22] discovered a CDA EST sequence (ES469341) when they investigated genes involved in gonad maturation of the scallop, *Argopecten purpuratus*. Wang et al. [23] reported a CDA EST

* Corresponding author. Tel.: +86 571 86971960; fax: +86 571 86971960.
E-mail address: wuxz@zju.edu.cn (X. Wu).

0145-305X/$ – see front matter © 2009 Elsevier Ltd. All rights reserved.
doi:10.1016/j.dci.2008.12.003

(EU244406) from a SSH cDNA libray of hemocyte in *Haliotsis diversicolor reeve*. However, these studies were just limited to the CDA gene investigations and little is known about the sequence property, biochemical or physiological functions of the CDA. In this report, a cDNA nucleotide sequence was selected from the abalone, *Haliotis diversicolor supertexta*, cDNA library. After sequence analyses, examination on expression pattern, identification of biological activity and determination of intracellular localization, we demonstrate that this gene is a novel CDA homologue, which we named ab-CDA.

2. Materials and methods

2.1. Animals, immune challenge and tissues collection

Healthy abalones (*H. diversicolor supertexta*) 3 years of age were collected from an abalone farm in Xiamen (Fujian, China) and kept in artificial seawater with a cycling system at 23 °C [24]. A minimum of 5 individuals was used in each experimental condition. Abalones were challenged by injecting 50 μL *E. coli* lipopolysaccharide (LPS) or viral mimic Polyriboinosinic polyribocytidylic acid (Poly I: C) (1 μg/μL diluted in sterile saline: 0.9% sodium chloride). In addition, abalones challenged with 50 μL autoclaved 0.9% sodium chloride were used as control. Hemocytes were collected at different times (0, 6, 12, 18, 24 h) post injection by centrifugation (700 × *g*, 10 min, 4 °C). Gills, digestive glands, foot muscle and mantle margin were also collected from healthy abalone without injection.

2.2. Preparation and screening of abalone cDNA library

Total RNA was isolated from challenged-abalone hemocytes using TRIzol reagent (Invitrogen, USA). Abalone cDNA library was constructed by a SMART™ cDNA library construction kit (Clontech, USA) according to the manufacture's instruction with a few modifications. Briefly, the isolated RNA was reverse-transcribed to synthesize first strand cDNA at 42 °C for 1 h. Then first strand cDNA was mixed with 5′PCR primer and other PCR reagents at 95 °C for 30 sec followed by 20 cycles of 95 °C for 10 s, 68 °C for 6 min to synthesize double-strand DNA. After digestion and purification, double-strand DNA was ligated to TriplEx2 Vectors. Then the resulting Ligation reaction was packed using the Lambda DNA Packaging System (Promega, USA) following the manufacturer's specifications. Screening of abalone cDNA library was based on polymerase chain reaction (PCR) with the pTriplEx2 sequencing primers shown in Table 1. Positive plasmid clones were grown in liquid cultures and induced to a high copy number for direct sequencing.

2.3. Sequence analysis and phylogenetic construction

Sequence analysis was carried out by BLAST software (www.ncbi.nlm.nih.gov/blast). Deduced amino acid sequences were aligned using ClustalW (http://npsa-pbil.ibcp.fr) software. Domain prediction was performed with SMART (http://smart.embl-heidelberg.de) software [25]. A phylogenetic tree was constructed based on full length amino acid sequences using the neighbor-joining method [26] and was drawn using MEGA version 3.1 [27].

2.4. Real-time PCR

Total RNAs from different tissues of healthy abalones or hemocytes of abalones challenged with LPS, Poly I: C, or equal volume of autoclaved 0.9% sodium chloride which were used as control were isolated using TRIzol reagent (Invitrogen, USA). The specific primers for ab-CDA and 28 s rDNA (Table 1) were designed by primer 3.0 software. Real-time PCR was performed using the SYBR Premix Ex Tag™ KIT (Takara, Japan). Briefly, the RNA was reverse transcribed into cDNA with M-MLV reverse transcriptase and the PCR reaction was performed in a 25 μL volume using a 7500 real-time PCR system (ABI, USA). Experiments were performed in triplicate and the data were represented as the mean ± SEM ($n = 3$) for Student's *t*-test analysis. Differences were considered statistically significant when p values were less than 0.05.

2.5. Protein expression and purification

Based on the entire ab-CDA coding region sequence, specific PCR primers (Table 1) were designed to amplify the mature protein. PCR products were digested with restriction enzymes (EcoRI, XhoI) and ligated to the PET-28 (a+) expression vector (Novagen, USA). After the recombinant plasmids were propagated in *E. coli* DH5a, they were transformed into *E. coli* BL21 (DE3) for protein expression. Then the recombinant fusion proteins were purified by affinity chromatography using the nickel-nitrilotriacetic acid agarose (Ni-NTA) resins (Qiagen, Germany) following the manufacturer's protocol. The purified recombinant protein was analyzed by 12% SDS-polyacrylamide gel electrophoresis at 25 mA for 2 h. The protein separation was visualized with Coomass brilliant blue R-250 (Sigma, USA). Molecular weight protein standards (Fermentas, USA) were used to determine the target protein size. Protein concentration was measured by the Bradford method [28].

2.6. Identification of ab-CDA

The ab-CDA fusion protein purified by affinity chromatography was excised from a 12% SDS polyacrylamide gel, reduced with an excess of dithiothreitol (DTT) and alkylated with iodoacetamide. The reaction products were treated with sequencing grade and modified trypsin (Promega, USA). The resulting peptides were desalted and concentrated on a Magic C18 (Michrom BioResources, USA) for Liquid Chromatography using a Michrom Paradigm MG4 system (Michrom BioResources, USA). The eluted peptide was used for electrospray ionization tandem mass spectrometry (MS) analyses on a LTQ-Orbitrap (Thermo Finnigan, USA). The scanning range of m/z was 300–2000, and the mass resolution R was 60,000.

Table 1
Primer sequences and their use.

Primer name	Nucleotide sequence (5′→3′)	Purpose
PTriplEx2-F	CTCCGAGATCTGGACGAGC	Sequencing primers for cDNA library
PTriplEx2-R	TAATACGACTCACTATAGGGC	
ab-CDA-F1	CTGTGTTCACAGGTTGCAATG	Real-time PCR expression analysis
ab-CDA-R1	GACCAGAGACTGTCGACACACG	
28SrDNA-F	GAATCCCTCATCCTAGCGA	Real-time PCR expression analysis
28SrDNA-R	CACGTACTCTTGAACTCTCTC	
ab-CDA-F2	ACGAATTCATGCCTGAATACAGCGAAG	Recombinant protein expression
ab-CDA-R2	ACCTCGAGTTAAGAATGCCCTGCTGTG	

2.7. Biological activity

The enzymatic activity of the recombinant fusion protein was determined by spectrophotometry as described previously with slight modification [29]. The reaction mixture (1 ml) containing 100 mM $KHPO_4$ (PH 7.5), 500 mM KCl, 0.2 mM cytidine (which is the natural substrate of CDA) and the appropriate ab-CDA fusion protein after purification was incubated at 37 °C for 1 h, and the reaction was terminated by adding 100 μl methanol and cooling on ice for 10 min. The concentration of substrate was determined at the wavelength of 286 nm.

2.8. Antibody preparation

Antibodies were prepared as previously reported [30]. In brief, purified proteins were homogenized in complete Freund's adjuvant (Sigma, USA). New Zealand White rabbits were immunized with purified proteins (2 mg for each rabbit) three times at 2-week intervals. Booster injections were given after another week with 1 mg purified proteins (diluted with incomplete Freund's adjuvant). Rabbit serum was collected 10 days after the last immunization. Antiserum was prepared according to the method described [31] and the titer was determined by enzyme-linked immunosorbent assay (ELISA), and stored at −80 °C.

2.9. Western blot analysis

25 μg purified recombinant proteins or proteins extracted from abalone hemocytes, gills and digestive glands were separated on 12% SDS/PAGE gels respectively and then transferred onto a polyvinylidene difluoride (PVDF) membrane by an electrophoretic transfer system (Bio-Rad, USA). Membranes were blocked for 1 h at room temperature with 5% skim milk in PBST and probed with prepared anti-CDA antibody or pre-immunized rabbit serum at 4 °C overnight respectively. Subsequently, the membranes were incubated with HRP-conjugated sheep anti-rabbit IgG antibody (Sigma, USA) for 1 h at room temperature. Immunoreactivity was detected with HRP-DAB Detection Kit (Tiangen, China). The anti-28 s antibody (Jingtian, China) was used as loading control.

2.10. Immunohistochemistry

Immunohistochemistry was performed as previously reported [32] with some modifications. Briefly, Paraffin-embedded sections were air dried at room temperature for 1 h, fixed in acetone for 10 min and then air dried for another 10 min. The sections were rinsed and rehydrated in phosphate-buffered saline (PBS) for 5 min. An indirect immunoperoxidase staining technique was performed with the ABC method by a commercial immunohistochemistry kit (BOSTER, China). Briefly, endogenous peroxidase was inhibited by treatment with 3% H_2O_2 in PBS for 30 min at 37 °C. Then blocking solution with 1.5% bovine serum albumin in phosphate-buffered (BSA/PBS) was applied to the sections for 20 min at room temperature to avoid non-specific binding of the biotinylated antibody. The prepared anti-CDA antibody and pre-immunized rabbit serum were added to the slides and incubated overnight at 4 °C

```
1       ACACACGGCAGATACCGTCGACAACAGCCGCCCACGGAACACACAGAGTCATGCCTGAAT
                                                      M  P  E  Y 4
61      ACAGCGAAGAACAACTTCAAAAGATCCTGAAGGCCAGCCATGAAGTAAAGAAAATGGCGT
          S  E  E  Q  L  Q  K  I  L  K  A  S  H  E  V  K  K  M  A  Y 24
121     ATTGCCCGTACAGCAAGTTCCCCGTCGGGGCAGCCCTTCTAACAGAAGACGGAACTGTGT
          C  P  Y  S  K  F  P  V  G  A  A  L  L  T  E  D  G  T  V  F 44
181     TCACAGGTTGCAATGTAGAAAATGCATCATATGGTCTGTCGATTTGCGCCGAGAGGACAG
          T  G  C  N  V  E  N  A  S  Y  G  L  S  I  C  A  E  R  T  A 64
241     CCATAGTCAAGGCCGTATCAGAAGGTCATCGGAAGTTCACGGCCATTGCCATCGCAAGCG
          I  V  K  A  V  S  E  G  H  R  K  F  T  A  I  A  I  A  S  D 84
301     ACATGAAAGAGATGATCGTACCCTGTGGCGTGTGTCGACAGTCTCTGGTCGAGTTTGGTG
          M  K  E  M  I  V  P  C  G  V  C  R  Q  S  L  V  E  F  G  V 104
361     TGGACTGGGATATGTATATGACGAAACCGGATATGACGTACAAAGTAATGAAAGTTAAGG
          D  W  D  M  Y  M  T  K  P  D  M  T  Y  K  V  M  K  V  K  E 124
421     AGTTACTTCCCTTAGCTTTTGTTCCAAGCGACCTTCAACGAGAGAGACTTCCGGCGAGAA
          L  L  P  L  A  F  V  P  S  D  L  Q  R  E  R  L  P  A  R  N 144
481     ACACAGCAGGGCATTCTTAAATAACAATTATCTGCACGCTTGTGACTTTGTGACCTCTGA
          T  A  G  H  S  *                                          149
541     TGAAGCAACATGGTGGCATATTCATCGTTTATAGAATATTTCCGATTTGTGCTCTTCACT
601     ATAGTTGTATCATACGCTTATCATTCAATTTCGGGCGATGGGGTCGTGGTTAACGCGCTC
661     GCTCGTCACTCTGTGGACAGGGTTCTATTCCTAAGATGTGTATAATCCATTTCTTGTGTC
721     CCCTGTGGTGATACTTCCAGAATATTGCGAAAAACGACGTAAAACTAAACTCACTCATTC
781     AGTTTGAGCCATGAATTGAAAGCGGCCATTTTGTTTCCCAACTTCTTGGCGAAGGAAAAC
841     TCCATACAACACAAATGCACTCTAGTACACCTTTTTCGTACAGGACCCGTGAAGGCCCGG
901     GCCAGAAGGTAATCTTCAGTGACCCATGTGTCGTAAAAGGCGACTAACGTGATCGGGTGG
961     TCAAGCTCTCTGACTATTTCACATATGGGTACAATGTGTGAAGCCTATTTCCGTGGTATT
1021    ATTGGAATATTGTCAAAGGCGGCGTAAAATGATACTCACTCAGTATAACAAAATCCGGCC
1081    TTGCAAGAAACACATTACAAGCAACTAGTAACCAATTCTTGTCGTAAGAGGCGACTCACT
1141    CACTCACTCACTCACTCACTCGCTCATTCTAGGCAGCCTGTACCCATGTTTCACTCTGAT
1201    TAATGTAGGGGCGGTGTGGTAGCCTAATGGTTAAAGCGTTGGCTCGTCACGCCGAAGACC
1261    CGGGTTCGAATTCCCACATGGGTACAATATGCGAAGCCCATTTCTGGTGTCCCCCGCCGT
1321    GATATTGCTGGAATATTGCAAAAAAACGGCGTGAAACCAAACTCAGTCCGTCAGTCTGAT
1381    TAATGTACAGTCAATACCTAGGTTTCAACGCGGGTGGGAGCTACGCATATACTCTGAGGT
1441    ATTTGTGGTTCGAATCAACCGCAGGTAGCTTTGTATGGAATCCACAGCTTATATTTAGAG
1501    GAATATCGAGTGTTTACCCGAATTATGACAAGTGCCTACTTGACTTGTTTCCATGACTTT
1561    TAAGACTTCTGTCCTGAATATGCTACTACGCTCCATTCTTTTGTGGAGACACCTTGTTTG
1621    TCAAATTCAGTATATAGAGGATGAAATTGCTTGGTTGCACTAAGTGTAAAACAGGGACCG
1681    GTGTTGTTCATGTATATCTGTGTTGATTAAACATTCTTTCGAAAAAAAAAAAAAAAAAAA
1741    AAAAAAAAAAAA
```

Fig. 1. Nucleotide and deduced amino acid sequences of ab-cDA from abalone, *H. diversicolor supertexta*. The translation start (ATG) and stop (TGA) codon are shaded. Possible mRNA instability motif ATTTA is underlined. The nucleotides are numbered along the left margin and amino acids are numbered along the right margin.

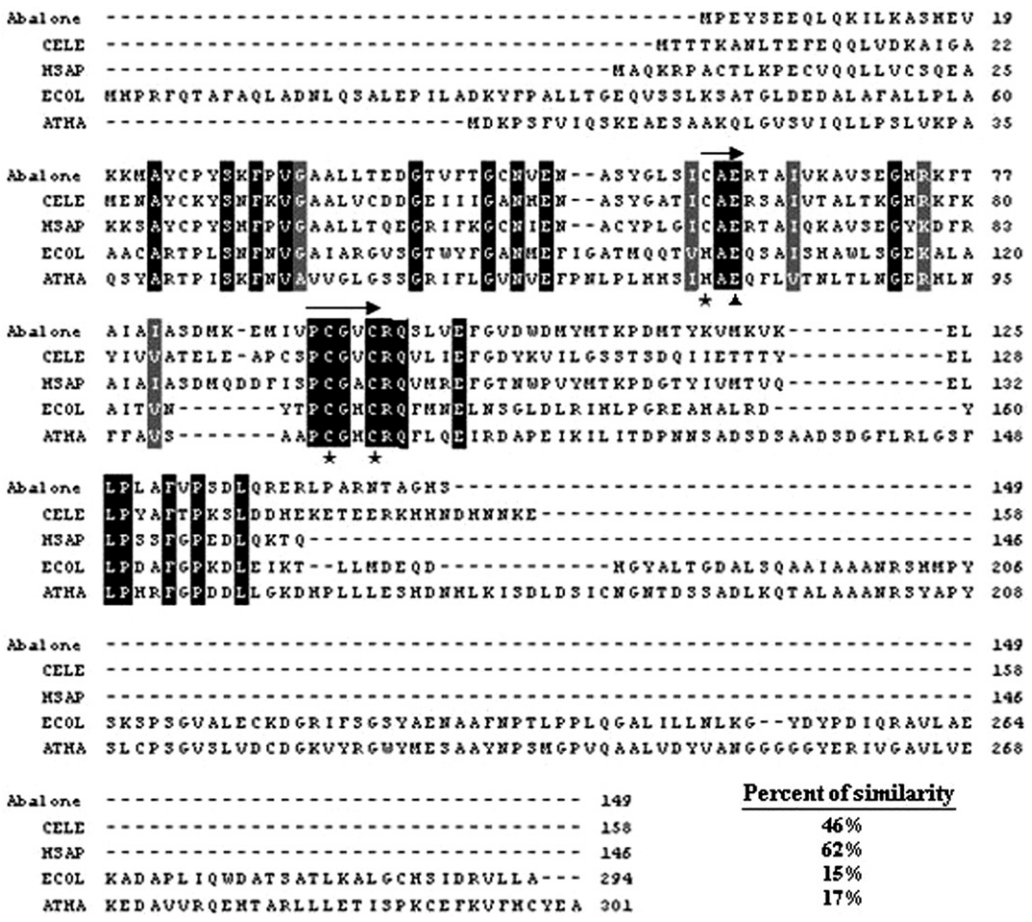

Fig. 2. Multiple amino acid sequences alignments between ab-CDA and other CDA members. Deduced amino-acid sequences of *Escherichia coli*, ECOL (NCBI accession number, P13652), *Arabidopsis thaliana*, ATHA (NCBI accession number, AJ005261), *Caenorhabditis elegans*, CELE (NCBI accession number, U64861), *Homo sapiens*, HSAP (NCBI accession number, P32320) and *Abalone* (NCBI accession number, EU101721) were aligned by Clustal program, version 1.83. Conserved amino acids are shaded and each shade represents a degree of conservation (black, 100%; gray 70%) The conserved active site domains are denoted by arrows above the sequences and the conserved cysteine/histidine residues involved in the Zn binding are denoted by asterisks. The conserved glutamate is denoted by triangle.

respectively. Goat anti-rabbit IgG antibody was added to the slides for 30 min at room temperature and peroxidase activity was visualized using a DAB kit (BOSTER, China). The reaction was stopped by rinsing in PBS after 15 min. Finally, the slides were mounted in aqueous-based mounting medium and examined by light microscopy.

3. Results

3.1. Sequence analysis of ab-CDA

A 1752-bp full length cDNA was obtained by screening an abalone cDNA library. The nucleotide and deduced amino acid

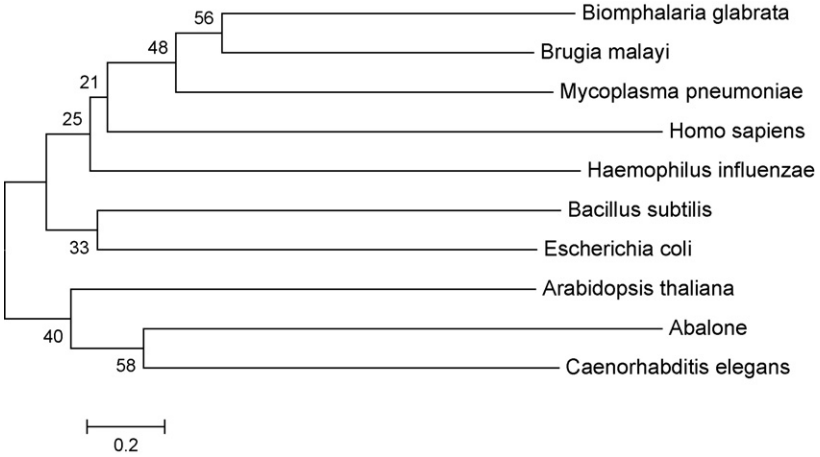

Fig. 3. Phylogenetic tree of representative CDA superfamily proteins. The neighbor-joining distance tree was constructed based on the entire amino acid sequence alignments of CDA superfamily proteins. Branch confidence levels (% based on 1000 bootstrap replicates) reveal an evolutionarily ancient split into the ab-CDA branch and other CDA member branches. NCBI accession numbers: *Escherichia coli* (P13652), *Arabidopsis thaliana* (AJ005261), *Haemophilus influenzae* (P44325), *Caenorhabditis elegans* (U64861), *Bacillus subtilis* (P19079), *Mycoplasma pneumoniae* (P75051), *Brugia malayi* (U80980), *Homo sapiens* (P32320), *Biomphalaria glabrata* (DQ117977) and *Abalone* (EU101721).

sequences of the full length cDNA are shown in Fig. 1. This cDNA has an ORF of 447 bp encoding 149 amino acid residues which has a predicted molecular weight of 16.6 kDa and PI of 7.3, respectively. The 5′ and 3′ untranslated regions (UTR) contain 50 and 1255 bp, respectively. A possible mRNA instability motif ATTTA at nucleotides 1492–1497 bp and a polyA tail in the 3′ UTR were identified. This cDNA sequence has been submitted to GenBank with accession no EU101721.

3.2. Characterization and homology comparison of ab-CDA

Based on the entire amino acid sequence, multiple alignments were performed using CDA homologues from different species (Fig. 2). Alignments with *Homo sapiens* CDA (62% similarity), *Caenorhabditis elegans* CDA (46% similarity), *Escherichia coli* CDA (15% similarity) and *Arabidopsis thaliana* CDA (17% similarity) show that the abalone protein contains two conserved active site domains and conserved cysteine/histidine residues involved in the Zn binding, which are the characteristics of CDA proteins. Thus, we believe that this abalone protein encodes a CDA homologue, which we named ab-CDA. The construction of an unrooted phylogenetic tree using the neighbor-joining method showed that the ab-CDA branched with *Caenorhabditis elegans* CDA and clustered with *Arabidopsis thaliana* CDA (Fig. 3).

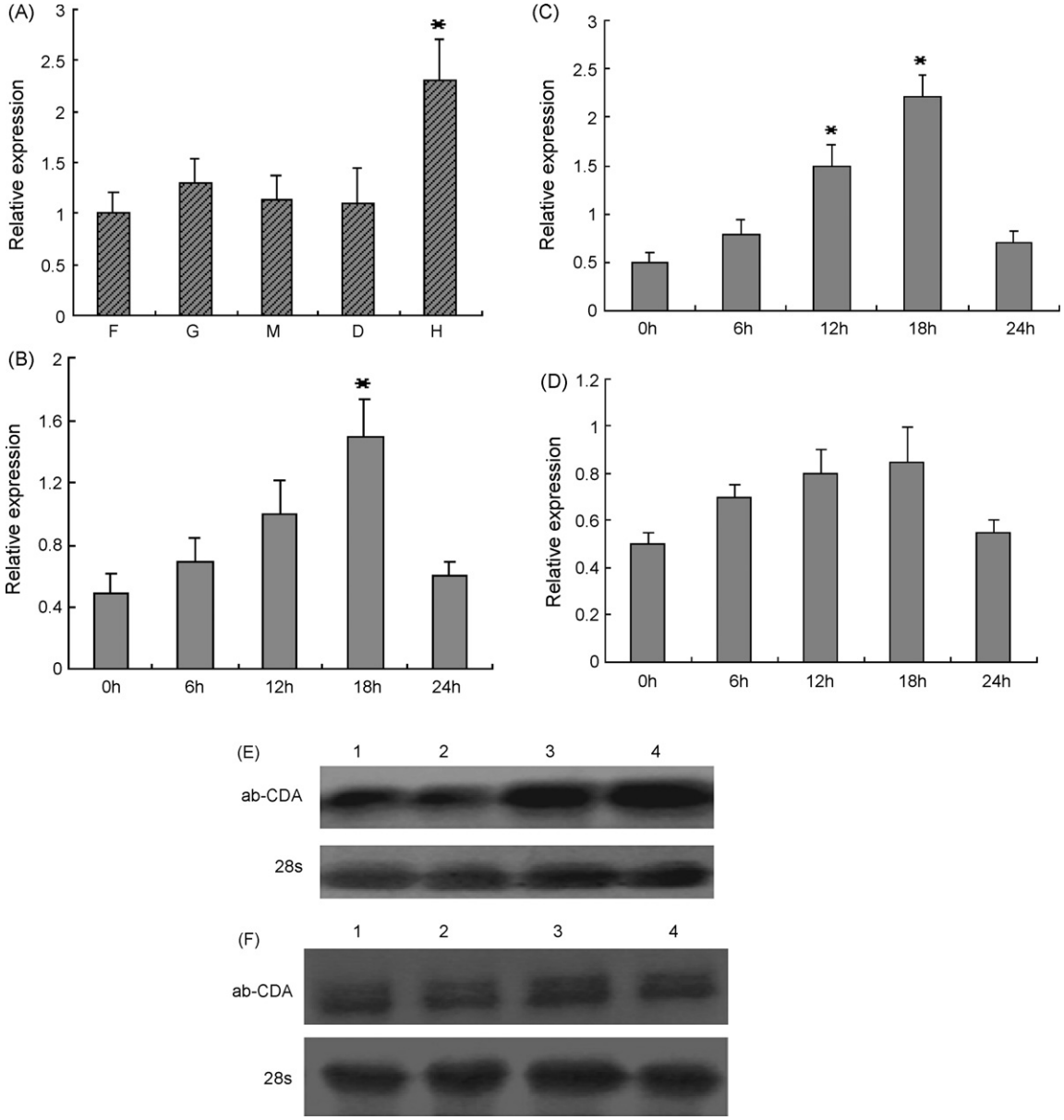

Fig. 4. (A) Expression levels of ab-CDA were detected in various tissues by real-time PCR. H: hemocyte; G: gills; D: digestive glands; M: mantle margin; F: foot muscle. Expression levels were assessed using the 28 s rDNA as endogenous control and the data were normalized by mRNA expression in the foot muscle. (B) Expression levels of ab-CDA in hemocyte at 0, 6, 12, 18 and 24 h after LPS challenge were detected by real-time PCR. (C) Expression levels of ab-CDA in hemocyte at 0, 6, 12, 18 and 24 h after Poly I: C challenges were detected by real-time PCR. (D) Expression levels of ab-CDA in hemocyte at 0, 6, 12, 18 and 24 h after 0.9% sodium chloride challenge were detected by real-time PCR and were used as control. The expression levels of 28 s rDNA were used as endogenous control. The values were presented as mean ± SEM ($n = 3$) and analyzed by Student's *t*-test. Asterisk indicates statistically significant difference ($P < 0.05$). (E) Expression levels of ab-CDA in hemocyte before and after LPS or Poly I: C challenges were detected by Western blot analysis. Lanes 1 and 2: expression level of ab-CDA in hemocyte before LPS or Poly I: C challenge; Lane 3: expression level of ab-CDA in hemocyte at 18 h after LPS challenge; Lane 4: expression level of ab-CDA in hemocyte at 18 h after Poly I: C challenge. (F) Expression levels of ab-CDA in hemocyte before and after 0.9% sodium chloride challenge were detected by Western blot analysis and were used as control. Lanes 1 and 2: expression level of ab-CDA in hemocyte before challenge; Lanes 3 and 4: expression level of ab-CDA in hemocyte at 18 h after challenge; 28 s was used as loading control.

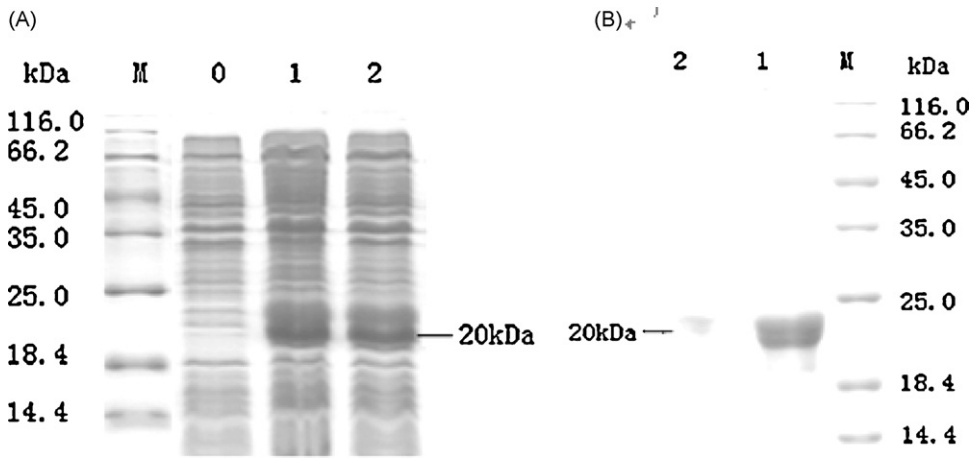

Fig. 5. (A) SDS-PAGE analysis of recombinant ab-CDA expressed in *E. coli*. Lane 0: lysate of *E. coli* without induction; Lane 1: recombinant ab-CDA expression induced by 0.5 mM IPTG; Lane 2: recombinant ab-CDA expression induced by 1 mM IPTG; M: unstained protein standards. The specific band of recombinant ab-CDA is indicated by lines. (B) SDS-PAGE analysis of purified recombinant ab-CDA. Lanes 1 and 2: purified recombinant ab-CDA; M: unstained protein standards. The protein separation was visualized with Coomass brilliant blue R-250.

MPEYSEEQLQKILKASHEVKKMAYCPYSKFPVGAALLTEDGTVFTGCNVENASYGLSICA
ERTAIVKAVSEGHRKFTAIAIASDMKEMIVPCGVCRQSLVEFGVDWDMYMTKPDMTYKV
MKVKELLPLAFVPSDLQRERLPARNTAGHS

Fig. 6. Characterization of ab-CDA by MS analysis. The peptide fragments of the protein identified by analysis of mass spectrometry data are underlined.

3.3. Expression analysis of ab-CDA

Real-time PCR analysis was performed to examine the expression of the ab-CDA transcript in different tissues: hemocyte, gills, digestive glands, foot muscle and mantle margin. It was shown that the ab-CDA was ubiquitously expressed in abalone tissues and a relatively high amount of ab-CDA transcript was observed in hemocyte (Fig. 4A). Real-time PCR analysis was also performed to examine whether LPS and Poly I: C had effects on the expression of ab-CDA in hemocytes. We observed that the expression levels of ab-CDA increased quickly after LPS and Poly I: C challenge (Fig. 4B and C) and reached their peak levels at 18 h. Furthermore, Poly I: C was more potent than LPS in up-regulating ab-CDA expression as the expression level was increased by three folds at 18 h during LPS challenge while the expression level was increased by four and a half folds at 18 h after Poly I: C challenge. Meanwhile, the difference is not significant in control group (Fig. 4D). Moreover, the results of Western blot analysis showed that the post-transcription level of ab-CDA was also increased after LPS and Poly I: C challenge (Fig. 4E) and no remarkable changes were revealed in control group (Fig. 4F).

3.4. Recombinant protein expression, purification and characterization

With the aim of identifying the function of ab-CDA, the ab-CDA protein was expressed as a fusion protein in *E. coli* (Fig. 5A) and purified by affinity chromatography. One single band with an apparent molecular mass of 20 kDa was shown by SDS-PAGE analysis (Fig. 5B). This is consistent with the predicted size of ab-CDA (16.6 kDa) and HIS (3.8 kDa) fusion protein. The protein was further confirmed by MS analyses. Thus four peptide fragments were unambiguously identified as tryptic fragments of the recombinant protein (Fig. 6). The sequence coverage of the matched protein was 35% overlapping with the amino acid sequence deduced from the ab-CDA.

3.5. Enzymatic activity

The ab-CDA showed conserved active site domains. We investigated whether ab-CDA had the characteristic of enzymatic activity as other CDA members using a spectrophotometric assay. The results showed that the efficiency of deamination was increased with increasing amounts of ab-CDA fusion proteins and leveled off at a concentration of 60 ng fusion proteins (Fig. 7). Thus we have demonstrated that the ab-CDA fusion protein can deaminate cytidine effectively.

3.6. Antibody preparation and Western blot analysis

We obtained a good antibody response with titers around 1:6000 (data not shown).

The specificity of the antibody was further analyzed by Western blotting. The results showed that a consensus protein of 20 kDa was detected in abalone tissues using the anti-CDA antiserum

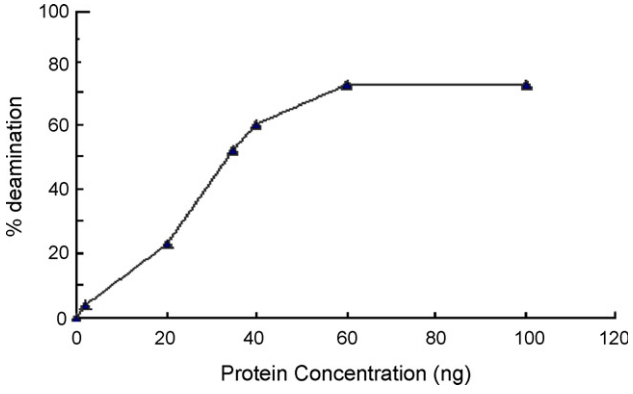

Fig. 7. Deaminase activity with increasing amounts of fusion protein. The activity was determined in vitro incubation with purified ab-CDA at 37 °C. The efficiency of deamination was increased with the accession of ab-CDA fusion protein until 60 ng.

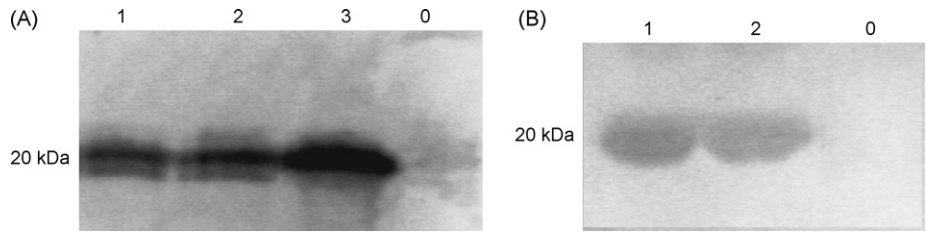

Fig. 8. (A) Western blotting analysis of ab-CDA in abalone tissues using the anti-CDA antibody. Lane 1: digestive glands; Lane 2: mantle margin; Lane 3: hymocyte; Lane 0: control. (B) Western blotting analysis of recombinant ab-CDA fusion protein using anti-CDA antibody. Lane 1 and 2: purified ab-CDA fusion protein; Lane 0: control. The expected bands of 20 kDa were detected using the anti-CDA antibody. No band was detected using the pre-immunized rabbit serum.

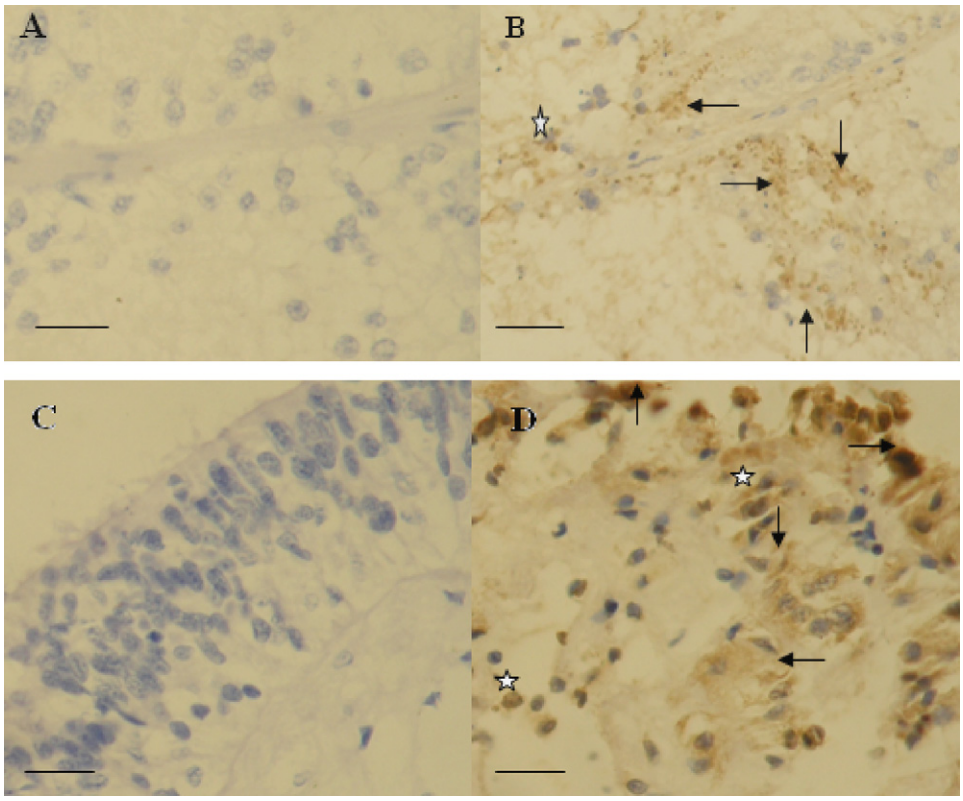

Fig. 9. Immunohistochemical labelling in digestive glands (A, B) and mantle margin (C, D) of abalone with the antibody against ab-CDA. (B) and (D) show the presence of ab-CDA in nucleus (asterisks) and cytoplast (arrows). Negative controls show no immunostaining signal (A, C). Scale bars: A, C, D, 80 μm; B, 100 μm.

(Fig. 8A). An immunoreaction was also detected against recombinant ab-CDA fusion protein (Fig. 8B). No immunoreactive band was detected in the control group using pre-immune rabbit serum. This demonstrated that the antibody was highly specific for ab-CDA.

3.7. *Intracellular localization of native ab-CDA*

Immunohistochemistry was performed using prepared antiserum to detect the intracellular localization of native ab-CDA in abalone tissues. The results exhibited strong staining in the cytoplast and relatively light staining in the nuclei (Fig. 9B and D). No immunostaining was detected in control samples (negative control) (Fig. 9A and C). These results suggested that ab-CDA is largely concentrated in the cytoplast and partially in the nuclei.

4. Discussion

In the present study, a full-length cDNA encoding ab-CDA protein was isolated from an abalone (*H. diversicolor supertexta*) cDNA library. We believe that ab-CDA is a CDA homologue for the following reasons: (1), ab-CDA shares high amino acid similarity with other CDA members; (2), ab-CDA shares conserved signature motifs with other CDA family proteins, including the zinc-binding region and active site domain; (3), ab-CDA has similar expression pattern to that of other CDA members; and (4), ab-CDA has a similar biological activity, catalyzing the model substrate of CDA.

The analysis of the ab-CDA amino acid sequence revealed that the abalone protein contains two conserved active site domains and conserved cysteine/histidine residues involved in the Zn binding, which are the characteristics of CDA protein family. Compared with other CDA members, the ab-CDA shares high amino acid similarity with homotetrameric members (62% similarity with *Homo sapiens* CDA and 46% similarity with *Caenorhabditis elegans* CDA) but relatively low amino acid similarity with homodimeric members (15% similarity with *Escherichia coli* and 17% similarity with *Arabidopsis thaliana*). In addition, the homodimeric members have one histidine and two cysteine residues liganding the zinc ion at the active sites while the three zinc ligands of the homotetrameric members are all cysteine residues [33]. We have shown that all cysteine residues liganding

the zinc ion at the active sites of ab-CDA are present (Fig. 2). Therefore, we suggest that the ab-CDA is a homotetramer protein that belongs to the homotetrameric class of CDA superfamily.

Real-time RT-PCR analysis revealed that ab-CDA was ubiquitously expressed in all examined tissues of abalone, which is consistent with the fact that ab-CDA is involved in a wide variety of biological processes [34]. Moreover, the expression level in hemocyte is higher than that of other tissues. It is known that hemocytes play a key role in the innate immune of invertebrate and carry out cellular responses towards microorganisms [35,36]. A relatively higher expression of ab-CDA was detected in normal hemocytes suggesting that ab-CDA may be involved in the immune response of abalone. To support this point, we performed another experiments to examine the expression changes of ab-CDA after LPS and Poly I: C challenge. Here we show that both LPS and Poly I: C can significantly up-regulate the expression level of ab-CDA, of which Poly I: C was apparently more potent. This also indicates that the expression of ab-CDA was differentially modulated by LPS and Poly I: C. Both LPS and Poly I: C are important structural motifs known as pathogen-associated molecular patterns (PAMPs) and the recognition for these structures can induce systemic inflammation and an immune response including the induction of pro-inflammatory cytokines and other anti-microbial genes [37–39]. LPS, as the best studied immuostimulatory component of bacteria, has been widely used as the model of infection and inflammation [37]. Poly I: C, a synthetic ligand for TLR3 that mimics the dsRNA produced during viral infection [38], has been also used to mimic viral infection and can stimulate antiviral activities of the innate immune system [40]. In addition, the leukocyte population is able to recognize and be activated by Poly I: C in fish [38]. The up-regulation of ab-CDA in hemocyte after LPS and Poly I: C challenge illustrated that it could occur immune response by the overexpression of ab-CDA in abalone hemocytes. Here we suggest that ab-CDA is involved in the immune response of abalone. However, the detailed mechanism for this up-regulation of ab-CDA induced by LPS and Poly I: C is still largely unknown. In addition, it was recently reported that DNA deamination can mediate innate immunity to retroviral infection through two possible mechanisms [41]. One is that deamination may lead to viral mutation and a high level of viral mutation may jeopardize viral expansion. The other is deamination may limit the spread of viral infection by triggering a uracil-based excision pathway. The present enzymatic activity study has shown that ab-CDA can catalyze the deamination of cytidine. So, we infer that the ab-CDA might play a role in innate immunity of abalone through its deamination based on the results that Poly I: C was more potent than LPS in up-regulating ab-CDA expression.

For the intracellular localization of CDA, Vincenzetti et al. [8] inferred that *Arabidopsis thaliana* CDA might be expressed in cytosol because it lacks a transit peptide for chloroplast or mitochondrial import. In contrast, Somasekaram et al. [34] believed that native human CDA was present in the nucleus as well as the cytoplasm in a variety of mammalian cells by immunochemistry analysis. And our results showed that ab-CDA is largely concentrated in the cytoplast and partially in the nuclei by immunohistochemistry analysis and further identified by Western blotting (data not shown). This fact that ab-CDA is largely concentrated in the cytoplast matches its function as an enzyme as the cytosol environment is required for enzyme activity. Meanwhile, the similarity of intracellular localization between ab-CDA and human CDA suggests that the same CDA class members may have similar intracellular localization. However, whether different intracellular localization from different CDA class members indicates different biological and physiological functions needs further investigation.

In summary, a novel CDA homologue from abalone has been identified based on nucleotide and amino acid sequences. The expression patterns, biological activity and intracellular localization of ab-CDA were characterized. The present functional characterization in vivo and vitro indicates that ab-CDA might be involved in the immune response of abalone. To our knowledge, this is the first report on the identification and functional characterization of a CDA homologue in the lower invertebrate abalone.

Acknowledgements

This work was supported by the National Natural Science Foundation of China (NFSC 30671619). We thank Dr. Yusheng Jiang and Yafeng Chen for their technical assistance and helpful suggestions.

References

[1] Cacciamani T, Vita A, Cristalli G, Vincenzetti S, Natalini P, Ruggieri S, et al. Purification of human cytidine deaminase: molecular and enzymic characterization and inhibition by synthetic pyrimidine analogs. Arch Biochem Biophys 1991;290:285–92.
[2] Wentworth DF, Wolfenden R. Cytidine deaminases (from *Escherichia coli* and human liver). Methods Enzymol 1978;51:401–7.
[3] Wisdom GB, Orsi BA. The purification and properties of cytidine aminohydrolase from sheep liver. Eur J Biochem 1969;7:223–30.
[4] Vincenzetti S, Cambi A, Neuhard J, Garattnni E, Vita A. Recombinant human cytidine deaminase: expression, purification, and characterization. Protein Expr Purif 1996;8:247–53.
[5] Müller WEG, Zahn RK. Metabolism of 1-β-D-arabinofuranosyluracil in mouse L5178Y cells. Cancer Res 1979;39:1102–7.
[6] Bouffard DY, Laliberté J, Momparler RL. Kinetic studies on 2′,2′-difluorodeoxycytidine (Gemcitabine) with purified human deoxycytidine kinase and cytidine deaminase. Biochem Pharmacol 1993;45:1857–61.
[7] Betts L, Xiang S, Short SA, Wolfenden R, Carter CW. Cytidine deaminase, the 2.3 Å crystal structure of an enzyme: transition-state analog complex. J Mol Biol 1994;235:635–56.
[8] Vincenzetti S, Cambi A, Neuhard J, Schnorr K, Grelloni M, Vita A. Cloning, expression, and eurification of cytidine deaminase from *Arabidopsis thaliana*. Protein Expr Purif 1999;15:8–15.
[9] Fleischmann RD, Adams MD, White O, Clayton RA, Kirkness EF, Kerlavage AR, et al. Whole-genome random sequencing and assembly of *Haemophilus influenzae* RD. Science 1995;269:496–512.
[10] Johansson E, Mejlhede N, Neuhard J, Larsen S. Crystal structure of the tetrameric cytidine deaminase from *Bacillus subtilis* at 2.0 Å resolution. Biochemistry 2002;41:2563–70.
[11] Chung SJ, Fromme JC, Verdine GL. Structure of human cytidine deaminase bound to a potent Inhibitor. J Med Chem 2005;48:658–60.
[12] Cambi A, Vincenzetti S, Neuhard J, Costanzi S, Natalini P, Vita A. Identification of four amino acid residues essential for catalysis in human cytidine deaminase by site-directed mutagenesis and chemical modification. Protein Eng 1998;11:59–63.
[13] Vita A, Cacciamani T, Natalini P, Ruggieri S, Raffaelli N, Magni G. A comparative study of some properties of cytidine deaminase from *Escherichia coli* and chicken liver. Comp Biochem Physiol B 1989;93:591–4.
[14] Vincenzetti S, Cambi A, Maury G, Bertorelle F, Gaubert G, Neuhard JP, et al. Possible role of two phenylalanine residues in the active site of human cytidine deaminase. Protein Eng 2000;13:791–9.
[15] Mangeat B, Turelli P, Caron G, Friedli M, Perrin L, Trono D. Broad antiretroviral defence by human APO-BEC3G through lethal editing of nascent reverse transcripts. Nature 2003;424:99–103.
[16] Dutko JA, Schäfer A, Kenny AE, Cullen BR, Curcio MJ. Inhibition of a yeast LTR retrotransposon by human APOBEC3 cytidine deaminases. Curr Biol 2005;15:661–6.
[17] Chiu LY, Greene WC. Multifaceted antivial actions of APOBEC3 cytidine deaminases. Trends Immunol 2006;27:291–7.
[18] Gordon HR, Cook PA. World abalone supply, markets and pricing: historical, current and future. J Shellfish Res 2001;20:567–70.
[19] Gardner GR, Harshbarger JC, Lake JL, Sawyer TK, Price KL, Stephenson MD, et al. Association of prokaryotes with symptomatic appearance of withering syndrome in black abalone *Haliotis cracherodii*. J Invertebr Pathol 1995;66:111–5.
[20] Moore JD, Robbins TT, Friedman CS. Withering syndrome in farmed red abalone, *Haliotis rufescens*. J Shellfish Res 1999;18:319–22.
[21] Bouchut A, Sautiere PE, Coustau C, Mitta G. Compatibility in the *biomphalaria glabrata/echinostoma caproni* model: potential involvement of proteins from hemocytes revealed by a proteomic approach. Acta Trop 2006;98:234–46.
[22] Boutet I, Moraga D, Marinovic L, Obreque J, Crooker PC. Characterization of reproduction-specific genes in a marine bivalve mollusc: influence of maturation stage and sex on mRNA expression. Gene 2008;407:130–8.
[23] Wang KJ, Ren HL, Xu DD, Cai L, Yang M. Identification of the up-regulated expression genes in hemocytes of variously colored abalone (*Haliotis diversicolor Reeve* 1846) challenged with bacteria. Dev Comp Immunol 2008;32:1326–7.
[24] Jiang YS, Wu XZ. Characterization of a Rel\NF-κB homologue in a gastropod abalone, *Haliotis diversicolor*. Dev Comp Immunol 2007;31:121–31.

[25] Schultz J, Milpetz F, Bork P, Ponting CP. SMART, a simple modular architecture research tool: identification of signaling domains. Proc Natl Acad Sci USA 1998;95:5857–64.
[26] Saitou N, Nei M. The neighbor-joining method: a new method for reconstructing phylogenetic tree. Mol Biol Evol 1987;4:406–25.
[27] Kumar S, Tamura K, Nei M. MEGA3: integrated software for molecular evolutionary genetics analysis and sequence alignment. Brief Bioinform 2004;5:150–63.
[28] Bradford MM. A rapid and sensitive method for the quantitation of microgram quantities of protein utilizing the principle of protein-dye binding. Anal Biochem 1976;72:248–54.
[29] Laliberté J, Marquez VE, Momparler RL. Potent inhibitors for the deamination of cytosine arabinoside and 5-aza-2′-deoxycytidine by human cytidine deaminase. Cancer Chemother Pharmacol 1992;30:7–11.
[30] Zhu BJ, Wu XZ. Identification of outer membrane protein ompR from rickettsia-like organism and induction of immune response in *Crassostrea ariakensis*. Mol Immunol 2008;45:3198–204.
[31] Harlow E, Lane D. Using antibodies: a laboratory manual. Cold Spring Harbor Laboratory Press; 1999.
[32] Selman L, Skjodt K, Nielsen O, Floridon C, Holmskov U, Hansen S. Expression and tissue localization of collectin placenta 1 (CL-PI, SRCL) in human tissues. Mol Immunol 2008;45:3278–88.
[33] Teh A, Kimura M, Yamamoto M, Tanaka N, Yamaguchi I, Kumasaka T. The 1.48 Å resolution crystal structure of the homotetrameric cytidine deaminase from mouse. Biochemistry 2006;45:7825–33.
[34] Somasekaram A, Jarmuz A, How A, Scott J, Navaratnam N. Intracellular localization of human cytidine deaminase. J Biol Chem 1999;274:28405–12.
[35] Bachere E, Gueguen Y, Gonzaiez M, Lorgeril J, Garnier J, Romestand B. Insight into the anti-microbial defense of marine invertebrates: the penaeid shrimp and the oyster crassostrea gigas. Immunol Rev 2004;198:149–68.
[36] Canesi L, Betti M, Ciacci C, Scarpato A, Citterio B, Pruzzo C, et al. Signaling pathways involved in the physiological response of mussel hemocytes to bacterial challenge: the role of stress-activated p38 MAPK. Dev Comp Immunol 2002;26:325–34.
[37] Lu YC, Yeh WC, Ohashi PS. LPS/TLR4 signal transduction pathway. Cytokine 2008;42:145–51.
[38] Sepulcre MP, Lopez-Castejon G, Meseguer J, Mulero V. The activation of gilthead seabream professional phagocytes by different PAMPs underlines the behavioural diversity of the main innate immune cells of bony fish. Mol Immunol 2007;44:2009–16.
[39] Meijer AH, Gabby Krens SF, Medina Rodriguez IA, He SN, Bitter W, Snaar-Jagalska BE, et al. Expression analysis of the Toll-like receptor and TIR domain adaptor families of zebrafish. Mol Immunol 2004;40:773–83.
[40] Fortier ME, Kent S, Ashdown H, Poole S, Boksa P, Luheshi GN. The viral mimic, polyinosinic:polycytidylic acid, induces fever in rats via an interleukin-1-dependent mechanism. Am J Physiol Regul Integr Comp Physiol 2004;287:759–66.
[41] Harris RS, Bishop KN, Sheehy AM, Craig HM, Petersen-Mahrt SK, Watt IN, et al. DNA deamination mediates innate immunity to retroviral infection. Cell 2003;113:803–9.